

Thermoelectric Power Studies of Ni-Co Nano Ferrites Synthesized By Citrate-Gel Auto Combustion Method

Abdul Gaffoor¹, D.Ravi Kumar³, G.Aravind², Ch .Abraham Lincoln³
D.Ravinder²

1.Lords Institute of Engineering and Technology,Hyderabad,Telangana-500008,India

2.Department of Physics, Osmania University, Hyderabad,Telangana-500007,India.

3Department of Chemistry, Osmania University, Hyderabad,Telangana-500007,India.

Abstract: One of the Electrical transport properties, Thermoelectric power of Co substituted Nickel Nano structured Ferrite materials with the formula $Ni_{1-x}Co_xFe_2O_4$, where ($x=0.0, 0.2, 0.4, 0.6, 0.8$ and 1.0) prepared by Citrate gel-auto combustion process were studied. The measurements were carried out from 320K to well beyond Curie temperature by the differential method. The Seebeck coefficient is negative for all compositions showing that these ferrites behave as n-type semiconductors. Plots of Seebeck coefficient verses temperature shows maximum at Curie temperature. On the basis of these results an explanation for the conduction mechanism in Ni-Co mixed ferrites is suggested. Compositional and temperature dependence of the Seebeck coefficient in the present ferrite system has been discussed. On the basis of these results a conduction mechanism for Ni-Co nano ferrites system is suggested in different temperature regions. The value of thermoelectric power shows maximum value at T_c (K).

Keywords: Ni-Co Nano Ferrites; Seebeck Coefficient; Conduction Mechanism; Curie Temperature

I. Introduction

Ferrites are low mobility semiconductors. Electrical transport properties of ferrites provide information suitable for the selection of these materials for specific application. To interpret the conduction mechanism in ferrites, Electrical transport properties such as Hall Effect and thermoelectric properties are widely used. Hall Effect measurement is straightforward and gives precise results. However, in case of ferrites that are low mobility semiconductors, it is somewhat difficult to measure the Hall Effect. In such cases the thermoelectric measurement is the only alternative. Moreover, the measurement of thermo e.m.f or seebeck coefficient is simple, straightforward and its sign gives vital information regarding the type of charge carriers (electrons and holes) responsible for the conduction process in semiconductors, i.e. whether they are n-type or p-type. It enables one to calculate Fermi energy, charge carrier concentration, mobility of charge carriers, etc [1,2]. Knowledge of Fermi energy gap helps in the determination of various regions namely impurity conduction, impurity exhaustion and intrinsic conduction regions of a semiconductor. The electron jumps between differently charged ions of the same metal present inequivalent crystallographic sites is responsible for the conduction in ferrites. Nickel and substituted nickel ferrite is one of the versatile and technologically important soft ferrite materials because of their typical ferromagnetic properties, low conductivity and thus lower eddy current losses, high electrochemical stability, catalytic behavior etc. [3-5]. The electrical transport properties of the ferrites are influenced by method of preparation, type of substituent, sintering temperature and duration [6]. Electrical and transport phenomena of Cd substituted Cobalt ferrites prepared by double sintering ceramic technique. were reported by A.M. Abdeen et al [7]. I.H. Gul et al have reported the magnetic and electrical properties of Zn substituted Co ferrites prepared by the chemical co-precipitation method [8].

During the past 10 years, considerable interest was observed in finding new materials and structures to make use in highly efficient cooling and energy conversion systems [9, 10]. To the best of author's knowledge no information is available on the high temperature thermoelectric power studies of Cobalt substituted Nickel nano ferrites synthesized by Citrate-gel method. Moreover, with a view to understand the conduction mechanism in Ni-Co nano ferrites system the investigation of thermoelectric power studies of $Ni_{1-x}Co_xFe_2O_4$ (with $x=0.0, 0.2, 0.4, 0.6, 0.8,$ and 1.0) nano ferrites prepared by Citrate-gel Method was undertaken. The present work reports the thermoelectric power and conduction mechanism of Cobalt substituted Nickel nano ferrites as a function of composition and temperature.

II. Materials And Methods

2.1 Materials

Ferrites with chemical formula $Ni_{1-x}Co_xFe_2O_4$ ($x= 0.0, 0.2, 0.4, 0.6, 0.8$ and 1.0) have been prepared by the Citrate-gel auto combustion method using Cobaltous Nitrate-($Co(NO_3)_2 \cdot 6H_2O$) (SDFCL-sd fine Chem.

Limited, 99% pure AR grade), Ferric Nitrate-(Fe(NO₃)₂9H₂O)(Otto Chemie Pvt. Limited, 98% pure GR grade), Nickel Nitrate - (Ni(NO₃)₂9H₂O)(Otto Chemie Pvt. Limited, 98% pure GR grade), Citric acid - (C₆H₈O₇.H₂O) (SDFCL-sd fine Chem. Limited, 99% pure AR grade), Ammonia - (NH₃) (SDFCL-sd fine Chem. Limited, 99% pure AR grade) as starting materials for the synthesis

2.2 Synthesis

Required quantities of metal nitrates were dissolved in a minimum quantity of distilled water and mixed together. Aqueous solution of Citric acid was then added to the mixed metal nitrate solution. Ammonia solution was then added with constant stirring to maintain P^H of the solution at 7. The resulting solution was continuously heated on the hot plate at 100°C upto dryness with continuous stirring. A viscous gel has resulted. Increasing the temperature upto 200°C lead the ignition of gel. The dried gel burnt completely in a self propagating combustion manner to form a loose powder. The burnt powder was ground in Agate Mortar and Pistle to get a fine Ferrite powder. Finally the burnt powder was calcined in air at 500°C temperature for four hours and cooled to room temperature.

2.3. Characterization

X-ray Diffraction with Cuka (lambda = 1.54 Å) was used to study the single phase nature and nano-phase formation of the Ni-Coferrite system at room temperature by continuous scanning in the range of 10°C to 90°C.

Micro structural analysis of the prepared samples was carried out by Transmission electron microscopy(TEM), scanning Electron microscopy (SEM) and elemental compositional analysis for all samples was done by Energy Dispersive Spectroscopy (EDS)

2.4 Method

For the thermoelectric power measurements, Circular pellets (diameter-13mm and thickness-2mm) of the synthesized powders were made using polyvinyl alcohol as binder by exerting a pressure of 5 tons for 1-2 minutes. These samples were finally sintered at 4000C for 5 hours and then slowly cooled to room temperature. Pellets were then coated with a thin layer of silver paste to have good electrical contact Thermo electric power studies on circular pellets of

Ni_{1-x}Co_xFe₂O₄ nano ferrites were measured by a differential method [11] from 320K to well beyond the Curie temperature. The sample was kept between the hot and cold junctions of the method in the form of pellet. The temperature difference between two ends of the sample was kept at 10K throughout the measured temperature range. A temperature difference maintained between the hot and cold surfaces of a sample results in the motion of electrons or holes. This leads to the development of a thermo e.m.f. across the sample which is measured by using a digital micro voltmeter.

The Thermoelectric power or Seebeck coefficient (S or α) was calculated using the relation

$$S = \frac{\Delta E}{\Delta T}$$

Where ΔE is the thermo e.m.f. produced across the sample as the charge carriers diffused from the hot to the cold surface due to a temperature difference ΔT in degree Kelvin across the sample.

III. Results And Discussions

3.1. XRD Analysis

The X-ray diffraction patterns of all the samples were shown in **Figure 1**. XRD patterns and the crystalline phases were identified by comparison with reference data from the JCPDS card No. 742081 for Nickel ferrites (NiFe₂O₄) and JCPDS card No 791744 for Cobalt ferrites (CoFe₂O₄). The XRD patterns of all the Cobalt substituted nickel ferrites showed a homogeneous single phased cubic spinel belonging to the space group Fd3m (confirmed by JCPDS card No. 742081). All the Bragg reflections have been indexed, which confirmed the formation of a well defined single phase cubic spinel structure without any impurity peaks. All the peaks are allowed peaks. The strongest reflection has come from (311) plane that indicates spinel phase.

The diffraction peaks can be indexed to the planes of (2 2 0), (3 1 1), (2 2 2), (4 0 0), (5 1 1) and (4 4 0). The observed broadening of diffraction peaks indicates the nano crystallinity of the samples. The particle size of the synthesized ferrite samples was estimated from X-ray peak broadening of diffraction peaks using Scherrer formula [12]. The values of the particle size, lattice constant and X-ray density as deduced from the X-ray data are given in Table 1

$$t = \frac{0.91\lambda}{\beta \cos \theta}$$

where λ = Wavelength of X-ray, β = Full width and Half Maxima in radians, θ = Bragg's angle at the peak position.

Lattice parameter "a" of individual composition was calculated by using the following formula and values were

tabulated in **Table 1**.

$$d = \frac{a}{\sqrt{h^2+k^2+l^2}}$$

where a = lattice parameter, d = inter planar distance, hkl = miller indices.

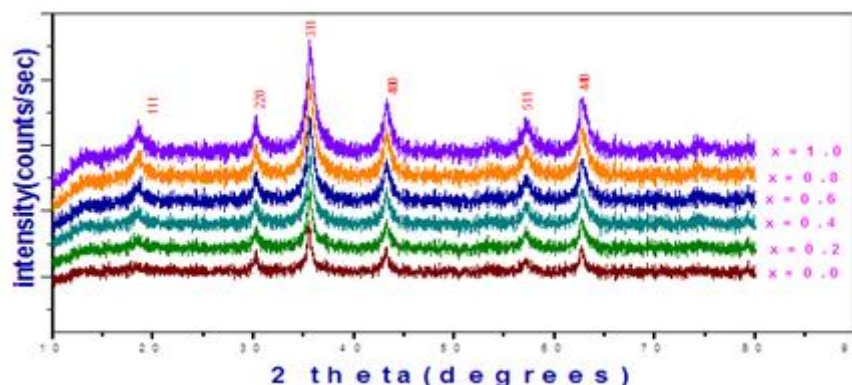


Figure 1. XRD of Ni_{1-x}Co_xFe₂O₄ (where x = 0.0, 0.2, 0.4, 0.6, 0.8, 1.0).

The lattice parameter was found to increase linearly with increasing Co concentration. This linear variation indicates that the Ni-Co ferrite system obeys Vegard’s law [13]. The lattice constant increases with Cobalt doping, which can be explained based on the relative ionic radius. The ionic radius (oct: 0.82 Å) of Co²⁺ ions is larger than the ionic radius (oct: 0.78 Å) of Ni²⁺ ions. Replacement of smaller Ni²⁺ cations with larger Co²⁺ cations causes an increase in lattice constant.

X-ray density (d_x) for different compositions was calculated using the formula [14] and calculated values were tabulated in Table 2.

$$d_x = \frac{ZM}{Na^3} \text{ gm/cc}$$

where Z = Number of molecules per unit cell (8), M = Molecular weight of the sample, N = Avogadro’s Number, a = lattice parameter.

Volume of unit cell was calculated by using the formula

V = a³ in Å³ units where ‘a’ is lattice parameter. Volume of unit cell was found to increase with increase in Co content, as it depends on lattice parameter which has increased with increase in Co content

The distance between magnetic ions (hopping length) in A site (tetrahedral) and B site (octahedral) were calculated using the relations

$$d_A = 0.25a\sqrt{3}, d_B = 0.25a\sqrt{2}$$

The calculated values of the hopping length for Tetrahedral site (d_A) and octahedral (d_B) of different compositions were tabulated in **Table 1**. It is observed that the hopping length increases as the Co content increases.

Table 1. Values of Crystallite size, Lattice parameter(a), unit cell volume, X-ray density and hopping length for A-Site(d_A) and B-Site(d_B) of Ni-Co Nano ferrite with Composition (X=0.0,0.2,0.4,0.6,0.8,1.0)

Sample	Particle size(nm)	Lattice parameter(A.u)	Unit cell volume(A.u)	X-Ray density(gm/cc)	A site d _A (A.u)	B Site d _B (A.u)
NiFe ₂ O ₄	23.57 nm	8.3422	580.552	5.362	3.6122	2.9494
Ni _{0.8} Co _{0.2} Fe ₂ O ₄	21.2 nm	8.3422	580.552	5.360	3.6122	2.9494
Ni _{0.6} Co _{0.4} Fe ₂ O ₄	20.37 nm	8.3576	583.773	5.359	3.6189	2.9548
Ni _{0.4} Co _{0.6} Fe ₂ O ₄	19.59 nm	8.3576	581.773	5.358	3.6139	2.9507
Ni _{0.2} Co _{0.8} Fe ₂ O ₄	12.19 nm	8.3576	583.773	5.337	3.6189	2.9548
CoFe ₂ O ₄	10.02 nm	8.3776	587.975	5.300	3.6276	2.9619

3.2 Morphology by TEM and SEM

Morphology of the prepared samples by Citrate-gel method was studied using Transmission electron microscope (TEM), Scanning electron microscope (SEM) where the secondary electron images were taken at different magnifications to study the morphology. The scanning electron microscopic images of all the synthesized samples were shown in **Figure 2**.

The images show that the particles have an almost homogeneous distribution, and some of them are in agglomerated form. It is evidenced by SEM images that the aggregation of particles lies in nano-metric region. The particles were observed as uniform grains (in different SEM images) confirming the crystalline structure of Ni-Co Nano ferrites which were detected by XRD studies. The formation of Fe₂O₄ was chemically favoured by heating during the synthesis where as final reaction was completed during the sintering where the pores between the particles were removed combined with growth and strong bonds by agglomeration.

It can be seen from SEM micrographs of various compositions that the morphology of the particles is similar. They reveal largely agglomerated, well defined nano particles of the sample powder with inhomogeneous broader grain size distribution. Such broader size distribution is characteristic of mechanically activated nano sized particles. The agglomeration of particles is also because they experience a permanent magnetic moment proportional to their volume [15].

Transmission Electron Microscopy (TEM) was performed for all the samples which is shown figure -3 and which indicates average particle size was ~20 nm. The particles were rounded in cubic shape and formed loose aggregates.

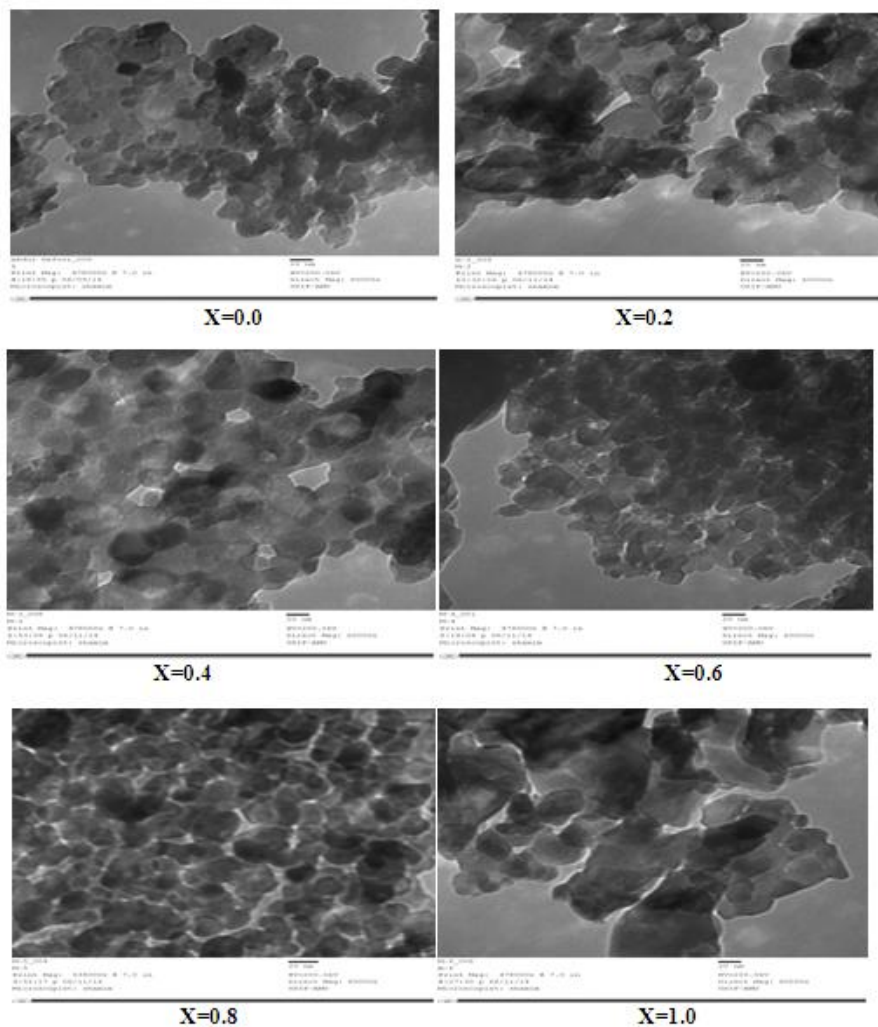


Figure2 TEM images of $Ni_{1-x}Co_xFe_2O_4$ Nano ferrites

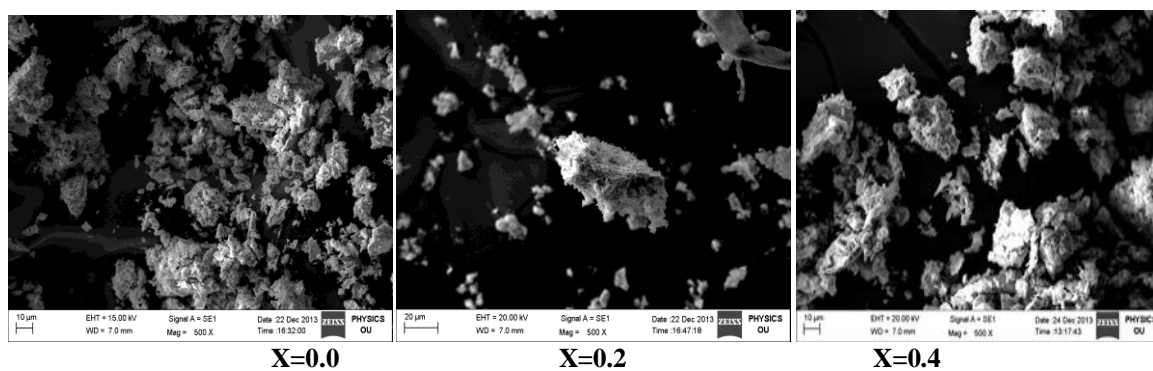


Figure 3 SEM images of $Ni_{1-x}Co_xFe_2O_4$ Nano ferrites

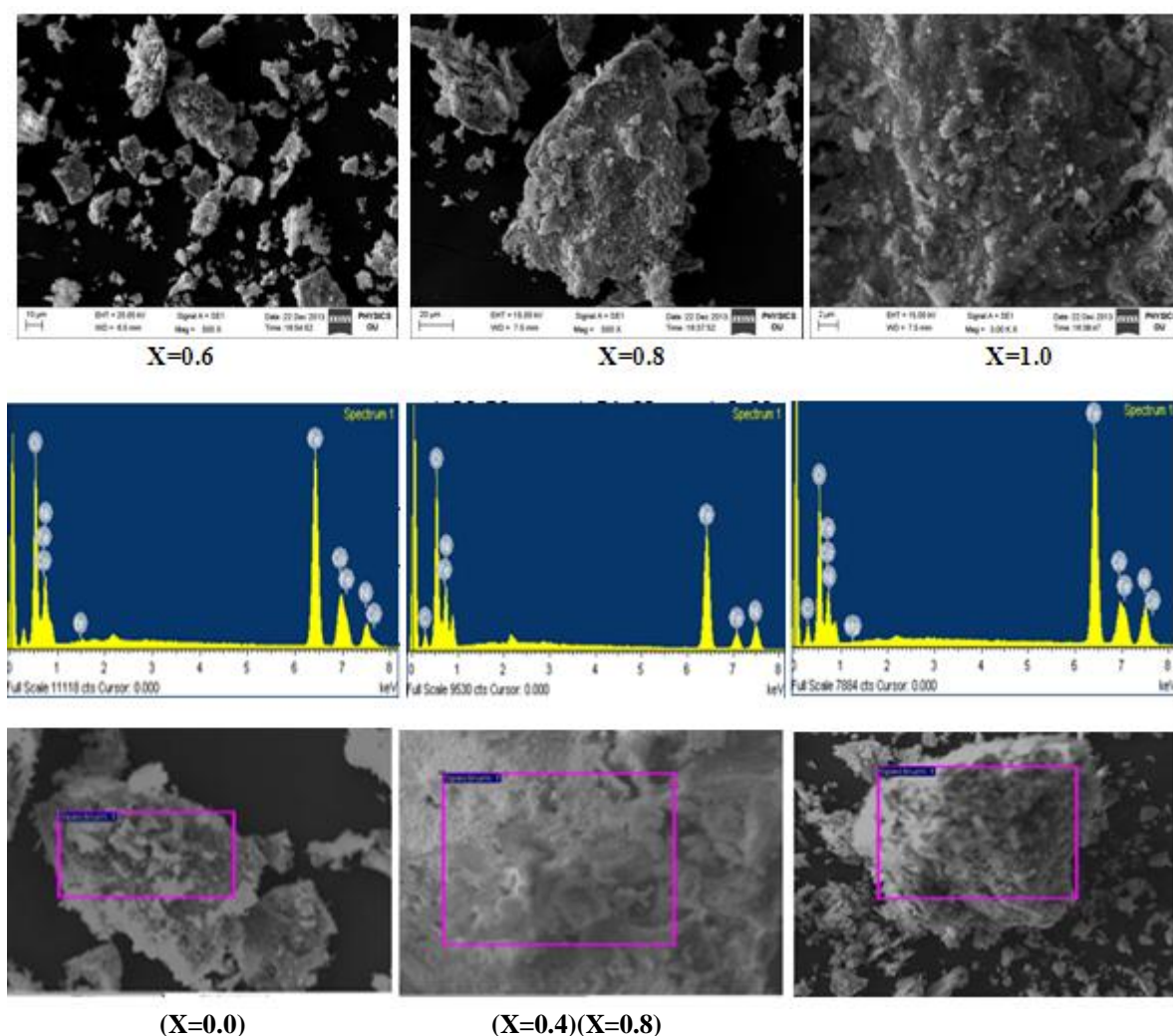


Figure-4EDS graph of $Ni_{1-x}Co_xFe_2O_4$ Nano ferrites with composition(X=0.0,0.4,0.8)

3.3. Elemental Analysis by EDS

The elemental analysis of all the Ni-Co nano ferrite samples with different compositions was analysed by Energy Dispersive Spectrometer (EDS) and the elemental % and atomic % of different elements in the were shown in the **Table 2**. The EDS pattern for samples with x = 0.0, 0.4 and 0.8 were shown in **Figure 4** which indicates the elemental and atomic composition in the sample. The compounds show the presence of Ni, Co, Fe and O without precipitating cations.

Table 2: Elements of each sample composition Ni-Co Nano ferrites analysed by (% weight) obtained by EDS

Element	O		Ni		Co		Fe	
	element%	Atomic %	element %	Atomic %	element%	Atomic %	Element %	Atomic %
$NiFe_2O_4$	29.93	61.88	18.12	9.50	-----	-----	51.92	28.62
$Ni_{0.8}Co_{0.2}Fe_2O_4$	21.85	49.77	19.31	12.00	6.00	3.71	52.83	34.52
$Ni_{0.6}Co_{0.4}Fe_2O_4$	28.97	59.23	9.11	5.07	14.91	8.28	46.35	27.15
$Ni_{0.4}Co_{0.6}Fe_2O_4$	33.38	42.77	12.15	5.70	9.18	4.29	45.28	41.24
$Ni_{0.2}Co_{0.8}Fe_2O_4$	33.53	51.63	2.69	0.91	11.26	3.80	52.50	43.66
$CoFe_2O_4$	34.56	66.10	-----	-----	10.88	9.50	46.62	24.34

3.4 Composition dependence of Seebeck Coefficient

The approximate Curie temperatures for the samples of the present ferrite system under investigation were measured using Loria technique and were tabulated in **Table 3**. Based on these values, Seebeck coefficient of the ferrite samples was measured from 320K to 800K (beyond Curie temperature). The values of Seebeck coefficient at 340K for the ferrite samples calculated from the measured values of thermo emf were reported in Table 3. It can be seen from the table that the sign of Seebeck coefficient for all the Ferrite samples is negative. Based on it, Ni-Co ferrites have been classified as n-type semiconductors at 340K.

Table 3: Thermoelectric power data of Ni-Co ferrites ($x=0.0, 0.2, 0.4, 0.6, 0.8, 1.0$) at 340K

Ferrite Composition	Seebeck Coefficient(S)($\mu V/K$) at 340K	Seebeck coefficient Curie Temperature	Loria Technique Curie Temperature
NiFe ₂ O ₄	-230	850	855
Ni _{0.8} Co _{0.2} Fe ₂ O ₄	-250	845	847
Ni _{0.6} Co _{0.4} Fe ₂ O ₄	-290	830	840
Ni _{0.4} Co _{0.6} Fe ₂ O ₄	-300	820	830
Ni _{0.2} Co _{0.8} Fe ₂ O ₄	-310	800	810
CoFe ₂ O ₄	-330	750	780

3.2 Temperature Dependence of Seebeck Coefficient

The variation of Seebeck coefficient (α) with hot junction temperature (T) for the different compositions of Ni_{1-x}Co_xFe₂O₄ ferrite system (with $x=0.0, 0.2, 0.4, 0.6, 0.8$ and 1.0) compositions were shown in Figures 5 to 10.

Figure 5 to 10 corresponds to Ni_{1-x}Co_xFe₂O₄ where ($x=0.0, 0.2, 0.4, 0.6, 0.8$ and 1.0) It can be seen from the figures that the sign of the Seebeck coefficients is negative in the measured temperature range indicating the n-type of semiconducting nature throughout this range. This means that the majority of charge carriers are electrons. Similar behavior of variation of Seebeck coefficient with temperature was observed in Ni-Cr ferrites [16].

With increase in temperature it is observed that magnitude of Seebeck coefficient increases in the ferromagnetic region and reaches a maximum at certain temperature, denoted as Seebeck coefficient transition temperature. However, beyond this transition temperature the value of Seebeck coefficient was found to decrease with further increase in temperature which is due to the magnetic transition where the material becomes paramagnetic. The transition temperatures of the ferrite samples measured from these figures were in good agreement with the Curie temperature values obtained from Loria method as evident from Table 1.

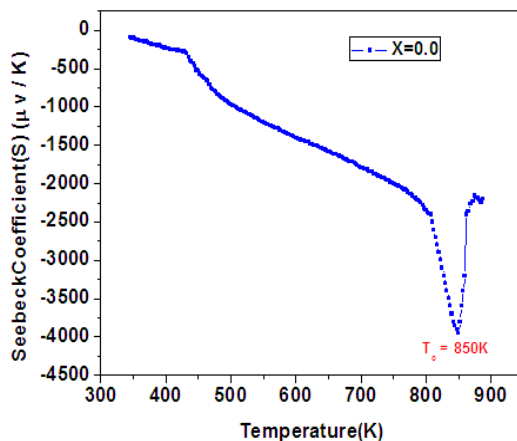


Figure-5: Plot of Seebeck Coefficient (S) versus temperature (T) for Ni_{1-x}Co_xFe₂O₄ (when $x=0.0$)

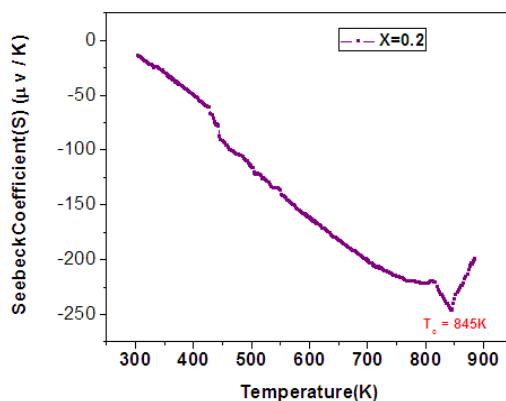


Figure-6 Plot of Seebeck Coefficient (S) versus temperature (T) for Ni_{1-x}Co_xFe₂O₄ (when $x=0.2$)

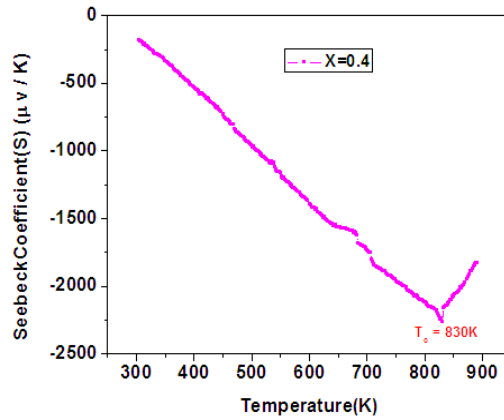


Figure-7:Plot of Seebeck Coefficient (S) versus temperature (T) for $\text{Ni}_{1-x}\text{Co}_x\text{Fe}_2\text{O}_4$ (when $x=0.4$)

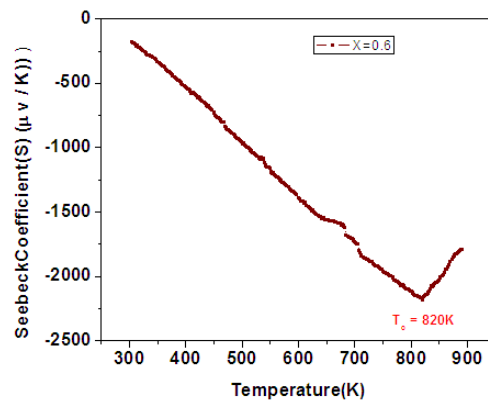


Figure-8:Plot of Seebeck Coefficient (S) versus temperature (T) for $\text{Ni}_{1-x}\text{Co}_x\text{Fe}_2\text{O}_4$ (when $x=0.6$)

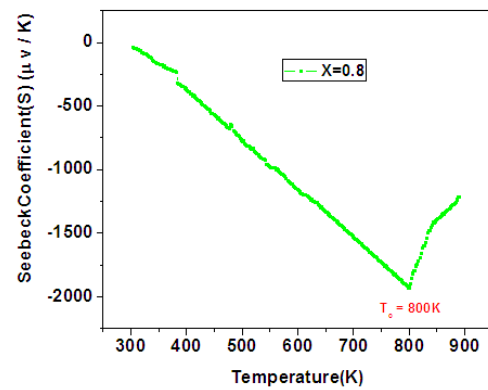


Figure-9:Plot of Seebeck Coefficient (S) versus temperature (T) for $\text{Ni}_{1-x}\text{Co}_x\text{Fe}_2\text{O}_4$ (when $x=0.8$)

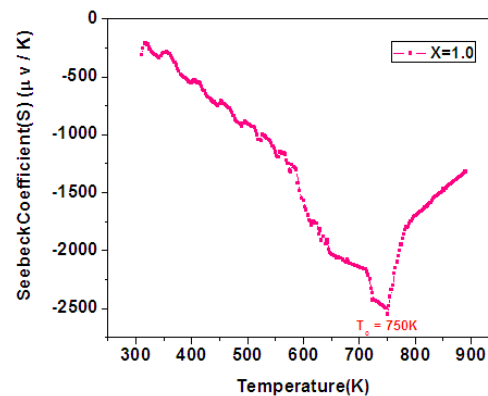
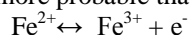


Figure-10:Plot of Seebeck Coefficient (S) versus temperature (T) for $\text{Ni}_{1-x}\text{Co}_x\text{Fe}_2\text{O}_4$ (when $x=1.0$)

This variation of Seebeck coefficient (α) with temperature can be explained based on the fact that in the case of n-type semiconducting materials (all the compositions of ferrites under investigation), the hot surface becomes positively charged, as it loses some of its electrons. The cold surface of the semiconductor becomes negatively charged due to the diffusion of free electrons from the hot portion. On increasing the temperature, the following conduction mechanism becomes more probable that generates electrons



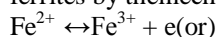
These electrons accumulate on the cold portion, as a result of which potential difference developed (ΔE) increases and Seebeck coefficient (α) increases. The decrease in Seebeck coefficient after the transition temperature may be due to filling up of oxygen vacancies and migration of ions from one site to other thereby reducing the concentration of mobile electrons [17].

Thus, it is clear that in case of Ni-Co ferrites the thermoelectric power (nonmagnetic property) is showing clear transition at the Curie temperature similar to the magnetic properties such as permeability, susceptibility and magnetization. It is clear from the figures that Seebeck coefficient is maximum at transition temperature (T_s).

This indicates that the magnetic ordering has marked influence on the thermoelectric property of the ferrites under investigation

3.3. Conduction mechanism

According to Verwey et al [18] the conduction mechanism in ferrites is due to exchange of electrons from the cations in the same site in the lattice. In Cobalt ferrites, the conduction can possibly be attributed to hopping of electrons between Fe^{2+} & Fe^{3+} as well as between Co^{2+} & Co^{3+} at the octahedral sites of the spinel ferrites by the mechanism



$\text{Co}^{2+} \leftrightarrow \text{Co}^{3+} + \text{e}^-$ At the tetrahedral sites, hole (e^+) is involved in hopping process between Co^{2+} and Co^{3+} by the hopping mechanism $\text{Co}^{2+} \leftrightarrow \text{Co}^{3+} + \text{e}^-$. As Co^{2+} ions cannot be formed on the B-sites, the probable conduction mechanisms in the system are $\text{Fe}^{2+} \leftrightarrow \text{Fe}^{3+} + \text{e}^-$ (n-type) at the B sites and $\text{Co}^{2+} \leftrightarrow \text{Co}^{3+} + \text{e}^+$ (p-type) at the A site of the spinel ferrite.

Assuming that two hopping mechanisms are involved, the predominance of one over the other depends upon the concentration of substituted cation $\text{Co}^{3+}(x)$ and temperature (T). If the electron exchange mechanism ($\text{Fe}^{2+} \leftrightarrow \text{Fe}^{3+} + \text{e}^-$) dominates to the hole exchange mechanism ($\text{Co}^{3+} \leftrightarrow \text{Co}^{2+} + \text{e}^+$) the ferrite composition might conduct as n-type semiconductor (or vice versa).

From **Figures 5 to 10**, the negative value of thermo electric power found over the entire measured temperature range shows that the majority of charge carriers are electrons. **Hence, the following conduction mechanism is suggested for all the samples of Ni-Co ferrites which is predominantly due to hopping of electrons [19] between Fe^{2+} and Fe^{3+} ions $\text{Fe}^{2+} \leftrightarrow \text{Fe}^{3+} + \text{e}^-$**

In ferrites, three regions were observed by number of researchers [20]. According to them, the conduction in the first region is due to the impurities, in second region due to polaron hopping and in third region it is due to magnetic ordering.

Thermoelectric effect is the direct conversion of temperature differences to electric voltage and vice versa. This effect can be used to generate electricity, measure temperature or change the temperature of objects. Thermoelectric devices can be used as temperature controllers because the direction of heating and cooling is determined by the polarity of the applied voltage.

IV. Conclusions

- Citrate Gel auto combustion technique is a convenient way for obtaining a homogeneous nano sized mixed Ni-Co ferrites.
- The process involves no impurity pickup and material loss. It is a very simple and economical method where no specific heating or cooling rate is required. It is a low temperature processing technique and requires shorter sintering duration.
- X-ray diffraction pattern confirms the formation of cubic spinel structure in single phase without any impurity peak. It is in good agreement with the standard data from ICSD
- The crystallite size of the various Ni-Co ferrites was in the range of 10-24 nm.
- The lattice parameter is increased with the increase of Co substitution in Ni-Co ferrites which indicates that the mixed Ni-Co ferrite system obeys Vegard's law.
- SEM micrographs of various compositions indicate the morphology of the particles is similar. They reveal largely agglomerated, well defined nano particles of the sample powder with inhomogeneous broader grain size distribution.

- Transmission Electron Microscopy (TEM) was performed for all the samples which indicates average particle size was ~20 nm. The particles were rounded in cubic shape and formed loose aggregates
- EDS data gives the elemental% and atomic % in the mixed Ni-Co ferrites and it shows the presence of Ni, Co, Fe and O without precipitating cations
- In the Ni-Co ferrite systems under investigation the Seebeck coefficient was found to increase with increase in Co composition indicating the generation of more and more n-type carriers
- In $\text{Ni}_{1-x}\text{Co}_x\text{Fe}_2\text{O}_4$ ($x=0.0, 0.2, 0.4, 0.6, 0.8$ and 1.0) all the samples behave as n-type semiconductor over the temperature range 340K to 800K
- In Ni-Co nano ferrite systems it is observed that with increase in temperature, the value of thermoelectric power increases and shows maximum value at curie temperature T_c (K) beyond which it decreases. Curie temperatures calculated from thermoelectric measurements were in agreement with those calculated from DC Resistivity measurements, Loria technique and with the reported values which decrease with increase in composition.

Acknowledgement

The authors are thankful to Prof. K.M. Jadhav, Department of Physics, Dr. B.A.M. University, Aurangabad, Maharashtra, India for providing facility for thermoelectric power measurements.

References

- [1]. S.A. Mazen and A. Elfalaky. Thermoelectric Power and Electrical conductivity of Cu-Ti Ferrite. *J MagnMagn Mater* 1999; 195:148
- [2]. V.K. Lakhani, K.B. Modi. Effect of Al³⁺ substitution on the transport properties of copper ferrite. *J Phys D: ApplPhys* 2011; 44: 245403.
- [3]. Sagar E. Shirsath, Santosh S. Jadhav, B.G. Toksha, S.M. Patange, K.M. Jadhav, *Scr.Mater.* 64 (2011) 773–776.
- [4]. JianzhenHuo, Mingzhen Wei, *Mater. Lett.* 63 (2009) 1183–1184.
- [5]. Muhammad Ajmal, AsghariMaqsood, *Mater. Lett.* 62 (2008) 2077–2080.
- [6]. A.K.M. AktherHossaina, S.T. Mahmuda, M. Sekib, T. Kawaib. H. Tabata. Structural, electrical transport and magnetic properties of $\text{Ni}_{1-x}\text{Zn}_x\text{Fe}_2\text{O}_4$. *J MagnMagn Mater* 2007; 312 : 210
- [7]. A.M. Abdeen, O.M. Hemeda, E.E. Assem and M.M. El-sehly. Structural, electrical and transport phenomena of Co ferrite substituted by Cd. *J MagnMagn Mater* 2002;238:75-83
- [8]. I.H. Gul, A.Z. Abbasi, F. Amin, M. Anis-Ur-Rehman, A. Maqsood. Structural, magnetic and electrical properties of $\text{Co}_{1-x}\text{Zn}_x\text{Fe}_2\text{O}_4$ synthesized by Co-precipitation method. *J MagnMagn Mater* 2007; 311: 494.
- [9]. M.M. Masada, M.A. Ahmed, M.A. El-Haiti, S.M. Atria. Semiconductive properties of Cu-Cr ferrites. *J MagnMagnMateri* 1995; 150: 51.
- [10]. O. Yamashita. Effect of linear and non-linear components in the temperature dependences of thermoelectric properties on the energy conversion efficiency. *EnerConvManag* 1968; 50:1968.
- [11]. V.D. Reddy, M.A. Malik and P.V. Reddy. Electrical Transport Properties of Manganese- Magnesium Mixed Ferrites. *Mater SciEng B* 1991; 8: 295.
- [12]. B. D. Cullity, “Elements of XR-Diffraction,” Addison Wesley Publishing, Reading, 1959, p. 132.
- [13]. L. Vegard, “The Constitution of Mixed Crystals and the Space Occupied by Atoms,” *Zeitschrift für Physics*, Vol. 5, No. 17, 1921, pp.17-23.
- [14]. R. C. kumbale, P. A. sheikh, S. S. Kamble and Y. D. kolekar, “Effect of Cobalt Substitution on Structural Magnetic and Electric Properties of Nickel Ferrite,” *Journal of Alloys and Compounds*, Vol. 478, No. 1-2, 2009, pp. 599-603. doi:10.1016/j.jmmm.2005.03.007
- [15]. Suryavanshi.S.S; Deshpand.V; Sawantn.S.R, *J. Mater. Chem. Phy.* 1999, 59, 199 Doi: 10.1016/S0254-0584(99)00046-2
- [16]. S. C. Chaudhari and A. K. Ghatage. Electrical and dielectric behavior of chromium substituted nickel ferrite. *Der ChemicaSinica* 2013;4: 47-51.
- [17]. B.L. Patil, S.R. Sawant, S.S. Suryavanshi and S.A. Patil. Conduction mechanism in Sn⁴⁺ substituted copper ferrite. *Bull Mater Sci* 1993;16:267
- [18]. Verwey E.J.W., Haymann P.W., Romejin F.C. Physical Properties and Cation Arrangement of Oxides with Spinel Structures II. Electronic Conductivity. *J ChemPhys* 1947; 15:181
- [19]. L.G. Van Uitert, Dc Resistivity in the Nickel and Nickel Zinc Ferrite System. *ChemPhys* 1955; 23:1883
- [20]. Kadam G.B., Shelke S.B. and Jadhav K. M. Effect of Zinc on A. C. Susceptibility and D. C. Resistivity of $\text{Ni}_{1-x}\text{Zn}_x\text{Fe}_2\text{O}_4$. *J Electron Elect Eng* 2010; 1: 3.